To optimize splice joint between different PCF-based devices and SMF transmission medium

Faramarz E. Seraji[1*] **and S. Farsinezhad**[2]

[1] *Optical Communication Group, Iran Telecom Research Center, Iran*

[2] *Electrical Engineering Department, Semnan University, Iran*

[*] *E-mail: feseraji@itrc.ac.ir*

Received April 21, 2008

An analysis of splice loss between photonic crystal fibers (PCFs) and conventional single-mode fibers (SMFs) is presented at bending and straight conditions, by using scalar effective index method (SEIM), vectorial effective index method (VEIM), and finite-difference frequency domain (FDFD) methods. It is shown that when there is a slight bending at the vicinity of splice joint, the spot size increases sharply at higher frequencies. On the basis of the obtained results, a mechanism to optimize the splice loss between PCFs and conventional SMFs, both with any geometry, is suggested. The results can be utilized for PCF-based devices to be jointed to SMF as a transmission medium.

OCIS codes: 230.0230, 240.0240, 000.4430, 060.2310, 060.2340.

doi: 10.3788/COL20090703.0246.

In the past several years, photonic crystal fibers (PCFs) have been under intense study for a number of unique and useful properties not achievable in conventional silica fibers. The development of PCFs has been limited by their fusion-splice to conventional devices which is due to the air holes in their claddings[1−7]. Most of the reports are based on experimental data obtained from fusion-splicing[1,4,5] and tapering methods[2]. A few numerical approaches on splicing of PCFs were reported, using finite-difference time-domain (FDTD) method[2,3]. In another report, a splice-free method was proposed for interfacing PCF and conventional single-mode fibers (SMFs)[6].

In this letter, we present a comparative analysis of splice joint of PCFs and SMFs, using fully vectorial effective index method (VEIM), scalar effective index method (SEIM), and FDFD method. On the basis of the obtained results, we propose a mechanism to optimize the splice loss between PCFs and SMFs with any geometry.

Parameters design of PCFs for single-mode operation is based on the calculation of its cladding effective index, defined as $n_{\rm SMF} = \beta_{\rm SMF}/k_0$, where $k_0 = 2\pi/\lambda_0$, $\beta_{\rm SMF}$ is the propagation constant, and λ_0 is the free space wavelength[8,9]. By considering an approximate step-index profile and Neumann boundary conditions in the Maxwell's equations, the characteristic equation of cladding fundamental mode, known as space filling mode, can be obtained by SEIM and VEIM methods, respectively[10,11], as

$$\frac{J_1(u')}{J_0(u)}\left[I_0(w) - \frac{N_0(u)\left[wI_1(w)J_0(u) + uJ_1(u)I_0(w)\right]}{u\left[J_1(u)N_0(u) - J_0(u)N_1(u)\right]}\right]$$

$$= -\frac{N_1(u')\left[wI_1(w)J_0(u) + uJ_1(u)I_0(w)\right]}{u\left[J_1(u)N_0(u) - J_0(u)N_1(u)\right]}, \qquad (1)$$

$$\left(\frac{P_l'(u)}{uP_l(u)} + \frac{I_l'(w)}{wI_l(w)}\right)\left(n_{\rm s}^2\frac{P_l'(u)}{uP_l(u)} + n_{\rm a}^2\frac{I_l'(w)}{wI_l(w)}\right)$$

$$= l^2\left(\frac{1}{u^2} + \frac{1}{w^2}\right)^2\left(\frac{\beta}{k}\right)^2, \qquad (2)$$

where $u = k_0 a\sqrt{n_{\rm s}^2 - n_{\rm eff}^2}$, $w = k_0 a\sqrt{n_{\rm eff}^2 - n_{\rm a}^2}$, and J's, N's, and I's are the first, second, and modified Bessel functions, $P(u) = J_l(u)N_l(ub/a) - N_l(u)J_l(ub/a)$ where $b \approx 0.525\Lambda$, $n_{\rm s}$ is the refractive index of silica and $n_{\rm a}$ is the refractive index of air, and a $(= d/2)$ is the air-hole radius. We present the simulation of cladding fundamental mode of a straight PCF using Eqs. (1) and (2) for $\Lambda = 2.3$ μm and different values of d, as shown in Fig. 1. When the air-hole sizes and the wavelength increase, the accuracy of SEIM method lowers down. The result obtained by VEIM for $n_{\rm SMF}$ is the same as that of the plane-wave method[12].

The VEIM method is a strong solver for space filling mode, but acts weak in describing $n_{\rm eff}$[13]. A suitable approach is FDFD method, based on discretization of electrical and magnetic fields, and averaging permittivity constants in two adjacent nodes of Yee's mesh[12].

By applying perfectly matched layer (PML) boundary conditions on Maxwell's equations, the effective refractive index of the core can be determined[14]. In Table 1, the results of simulations of a straight PCF for $\Lambda = 6.75$ μm and $d = 2.5$ μm obtained by the four methods are

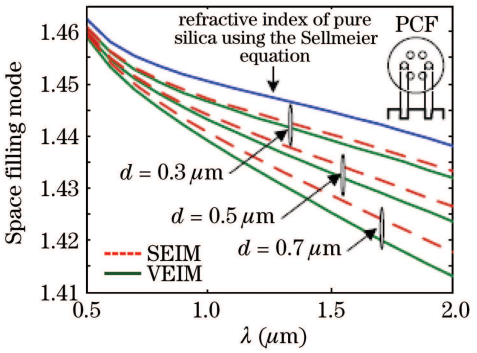

Fig. 1. Space filling mode versus wavelength using SEIM and VEIM methods for different values of d at $\Lambda = 2.3$ μm.

Table 1. Different Values of $n_{\rm eff}$ Obtained by Different Methods

λ (nm)	SEIM	VEIM	FDFD	FEM[13]
1450	1.44761	1.44720	1.44534	1.44539
1550	1.44729	1.44685	1.444698	–

compared. It shows that the methods SEIM and VEIM in determining $n_{\rm eff}$ for higher wavelength are less accurate.

The spot size which determines the bending loss and the loss at the splice joint may be represented by Petermann II expression given by[15]

$$W_{\rm PII} = a_{\rm eff}\sqrt{2}\left[\frac{J_1(U_{\rm eff})}{W_{\rm eff}J_0(U_{\rm eff})}\right], \quad (3)$$

where J's are the Bessel functions of zero and first orders, $a_{\rm eff}$ is the effective PCF radius, $U_{\rm eff}$ and $W_{\rm eff}$ are the PCF parameters defined as

$$U_{\rm eff} = k_0 a_{\rm eff}\sqrt{n_{\rm co}^2 - n_{\rm eff}^2},$$

$$W_{\rm eff} = k_0 a_{\rm eff}\sqrt{n_{\rm eff}^2 - n_{\rm SFM}^2}, \quad (4)$$

$n_{\rm co}$ is the core refractive index, $n_{\rm SFM}$ is the refractive index of space filling mode. Based on Eq. (3), Fig. 2 illustrates the spot size versus normalized frequencies ($V_{\rm SMF}$ and $V_{\rm PCF}$) of SMF and PCF for different values of d/Λ. It shows that when d/Λ varies from 0.1 to 0.7, the maximum normalized frequency changes from 1.2 to 4.8. The corresponding spot sizes change with the same trend as that of $V_{\rm PCF}$. When the normalized frequency increases, the spot size will reduce[10,16].

Since our proposed mechanism is based on a bending structure of spliced fibers, we should determine the values of $n_{\rm SMF}$ and $n_{\rm eff}$ for the bent PCF using

$$n_{\rm b}^2(x,y) = n_{\rm st}^2(x,y)(1+2y/R), \quad (5)$$

where $n_{\rm b}(x,y)$ denotes the effective index of bent PCF in the y direction with bending radius of R and $n_{\rm st}(x,y)$ indicates the effective index of the straight PCF[11].

The spot size of the bent PCF for the value of $n_{\rm SFM}$ should be determined. The effective refractive index of cross section of the bent PCF along the y axis, based on Eq. (5), is plotted in Fig. 3. When the bending radius decreases, the effective index increases linearly. From

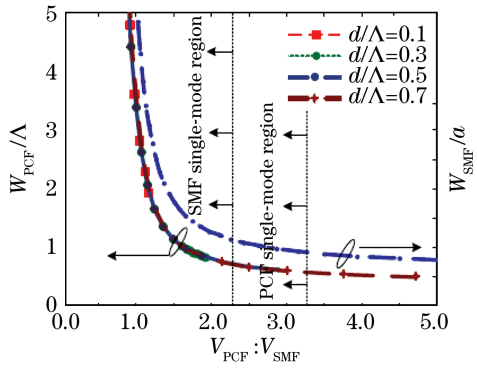

Fig. 2. Dependence of spot size on normalized frequency and single-mode regions of straight SMF and PCF fibers.

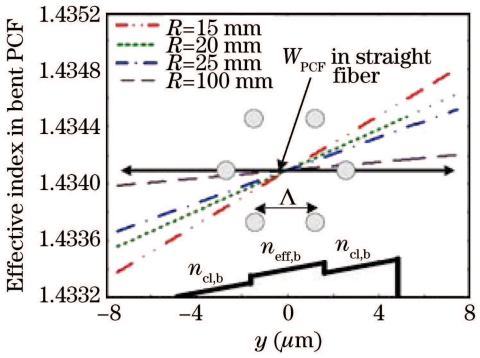

Fig. 3. Effective index of bent and straight PCFs for $\Lambda = 2.3$ μm and $d = 0.35$ μm at $\lambda_0 = 1550$ nm.

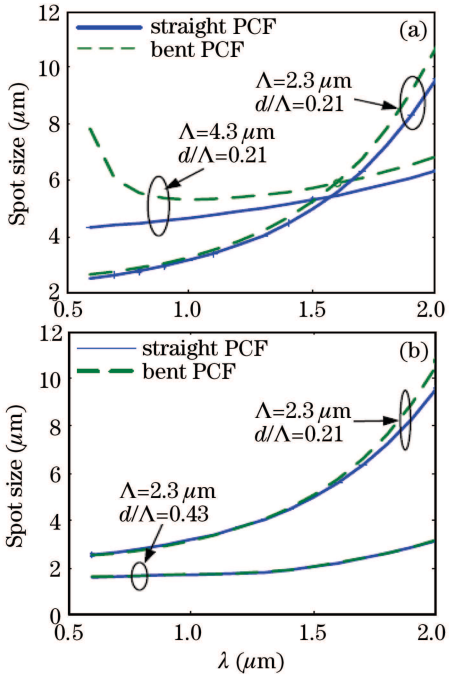

Fig. 4. Spot sizes of bent and straight PCFs versus λ for (a) different Λ and (b) different d/Λ at $R = 1$ cm.

Figs. 2 and 3, the spot size of the bent PCF can be evaluated.

Spot sizes of bent and straight PCFs versus wavelength for different Λ and d/Λ are plotted in Fig. 4 at $R = 1$ cm, which shows that by bending the PCF, the spot size would increase. In Fig. 4(a), by increasing Λ for a constant d/Λ, the spot size increases at some lower wavelengths and decreases at some higher wavelengths, due to dependency of $w_{\rm PCF}$ on $V_{\rm PCF}$, as shown in Fig. 2. At 1520 nm, the increase of Λ has no effect on the spot size for $d/\Lambda = 0.21$. By the increase of d/Λ with a constant Λ, the spot size reduces, as shown in Fig. 4(b). Comparing Figs. 4(a) and (b), we observe that the effect of Λ variation on spot size is more than that of d, which is due to the dependency of slope of refractive index on wavelength. As a result, if a constant d/Λ is considered, a higher Λ value rather than a lower d will be preferable in adjusting the spot sizes of spliced fibers while using our proposed mechanism. At higher values of Λ, the difference between spot sizes of bent and straight PCFs increases more. For instance, for $\Lambda = 2.3$ μm, the difference is 0.29 μm, and for $\Lambda = 4.3$ μm, the difference

is 0.43 μm, indicating 48% increase.

When there is no misalignment at the joint between PCF and SMF, the loss due to spot sizes is given as[9]

$$\alpha_n(\mathrm{dB}) = -20\log\left[\frac{2W_{\mathrm{PCF}}W_{\mathrm{SMF}}}{(W_{\mathrm{PCF}}^2 + W_{\mathrm{SMF}}^2)}\right], \quad (6)$$

where W_{SMF} and W_{PCF} are the spot sizes of SMF and PCF, respectively.

In a splice, there are three cases of $W_{\mathrm{SMF}} = W_{\mathrm{PCF}}$, $W_{\mathrm{SMF}} > W_{\mathrm{PCF}}$, or $W_{\mathrm{SMF}} < W_{\mathrm{PCF}}$. Figure 5(a) shows the splice loss and power coupling of a PCF (with $\Lambda = 6.41$ μm, $d/\Lambda = 0.345$) spliced to Corning SMF-28e fiber (with radius $a = 4.1$ μm) as a function of Λ for Petermann II and Gaussian beam spot sizes. At $\Lambda = 2.4$ and 6.41 μm, there are two minima for the loss, where at the former Λ value, the PCF core becomes unequal to the SMF core, but at the latter value, the cores of two fibers are equal. Then, every straight standard SMF can only be spliced to a particular straight PCF with a minimum splice loss. Figure 5(b) shows the corresponding curves in terms of d/Λ for two different PCFs and SMFs. For higher values of Λ and a, the splice loss becomes higher. We note that the splice losses between the PCFs having Λ in the range of $6.41 - 7.81$ μm and SMFs with a radius in the range of $4.1 - 5$ μm are at minimum. For a perfect splice, the loss at the joint is about 0.03 dB. The results for Petermann II and Gaussian beam spot sizes are almost the same.

When $W_{\mathrm{SMF}} > W_{\mathrm{PCF}}$ and $W_{\mathrm{SMF}} < W_{\mathrm{PCF}}$, there will be splice loss between two spliced fibers. To compensate the splice losses in these cases, we consider to develop the bending at the joint splice, as shown in Fig. 6. The intensities in the bent fibers become unsymmetrical with respect to the central axis[11], as shown in Fig. 7, that is plotted for SMF-28e with core radius of 4.1 μm and numerical aperture NA = 0.12[17] and in straight and bent PCFs with $\Lambda = 6.41$ μm and $d/\Lambda = 0.345$.

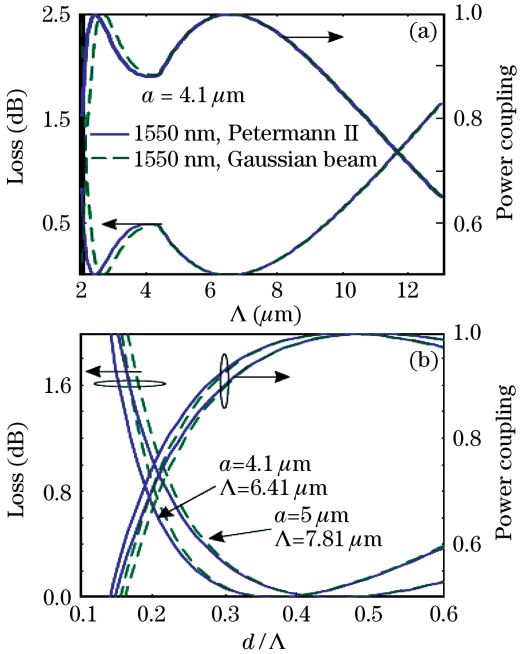

Fig. 5. Optimized values for splice loss and power coupling between SMF and PCF versus (a) Λ and (b) d/Λ for two different PCFs and SMFs at $\lambda = 1550$ nm.

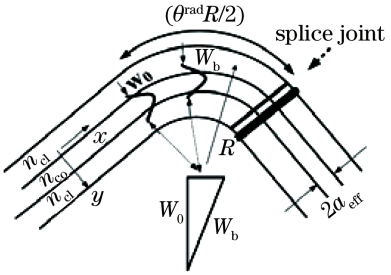

Fig. 6. Bending developed at the splice joint. θ is the bending angle in radians and a_{eff} is the effective core radius.

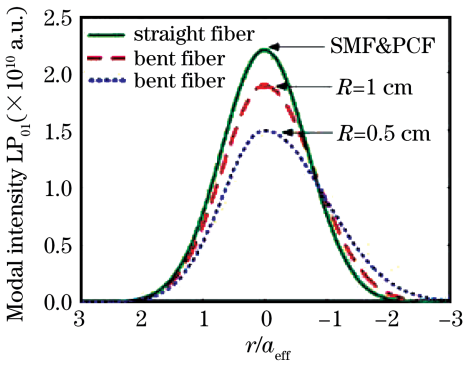

Fig. 7. Effects of bending of PCF on light intensities.

It is observed that the intensities of straight SMF-28e and PCF almost coincide with each other. In a bent PCF, as the bending radius increases, the spot size stretches towards opposite bending direction, i.e., the light intensities in the bent fibers become unsymmetrical with respect to the central axis[11].

Based on our calculations, the spot sizes of straight SMF and PCF are found as 5.14 and 5.15 μm, respectively. For the bent PCF, the spot size increases by 0.18 μm.

The loss created at the splice joint due to a displacement of bent fibers at the joint is obtained as

$$L_u = -10\log\left\{\left[\frac{2W_{\mathrm{SMF}}W_{\mathrm{PCF}}}{(W_{\mathrm{SMF}}^2 + W_{\mathrm{PCF}}^2)}\right]^2 \times \exp\left[-\frac{2u^2}{W_{\mathrm{SMF}}^2 + W_{\mathrm{PCF}}^2}\right]\right\}, \quad (7)$$

where u is the intensity displacement due to unsymmetrical spot sizes. Now, on the basis of the obtained results, if two spliced fibers have unequal spot sizes, we can adjust the size by bending one of the fibers. For alignment of equalized spot sizes of spliced fibers, we can apply the lateral displacement.

The permissible bending loss of a PCF in dB/km is obtained as[18]

$$\alpha\Lambda = \frac{8.686\Lambda\lambda}{8\sqrt{6\pi}A_{\mathrm{eff}}n_{\mathrm{s}}}\frac{1}{\sqrt{x}}F(-x),$$

$$x = \frac{R\lambda^2}{6\pi^2 n_{\mathrm{s}}^2\Lambda^3}V_{\mathrm{PCF}}^3,$$

$$V_{\mathrm{PCF}} = \frac{2\pi}{\lambda}a_{\mathrm{eff}}\sqrt{n_{\mathrm{co}}^2 - n_{\mathrm{SFM}}^2}, \quad (8)$$

where $A_{\rm eff}$ is the effective core area of PCF and R is the bending radius whose critical value is $R_{\rm c} \approx \Lambda^3/V_{\rm PCF}^3$, and $n_{\rm s}$, $n_{\rm co}$, $n_{\rm SFM}$, and $a_{\rm eff}$ are the refractive indices of silica, core, space filling mode, and the effective core radius, respectively[18].

The bending loss variation shows that for a constant Λ (Fig. 8(a)) and d/Λ (Fig. 8(b)), the bending loss decreases by increasing the wavelength. At longer wavelengths, the effect of d/Λ variation on loss is negligible and more loss develops at shorter wavelengths. For example, at 800 nm, for $R = 1$ cm, $\Lambda = 2.3$ μm, and $d/\Lambda = 0.2$ and 0.3, the losses are about 31 and 44 dB/km, respectively. In Fig. 6, the distance traveled by the light energy through the bent fiber is found as $\theta^{\rm rad}R/2$. At 1550 nm, the loss in PCF with $\Lambda = 2.3$ μm and $d = 0.5$ μm for $R = 1$ cm is $7.6 \times 10^{-5}\theta^{\rm rad}$ dB and for $R = 0.5$ cm is $4.99 \times 10^{-4}\theta^{\rm rad}$ dB.

Figure 9 shows the spot sizes of SMF-28e with NA = 0.12 and a typical PCF with $\Lambda = 2.3$ μm and $d = 0.5$ μm versus wavelength for $R = 1$ cm. It shows that for some wavelengths the spot size of bent PCF equals that of straight SMF while at other wavelengths the spot size of straight PCF coincides with that of bent SMF. To implement this scheme, given in Figs. 8 and 9 one has to find the detrimental parameters such as bending radius, bent spot sizes, and bending angle of the fiber from straight position.

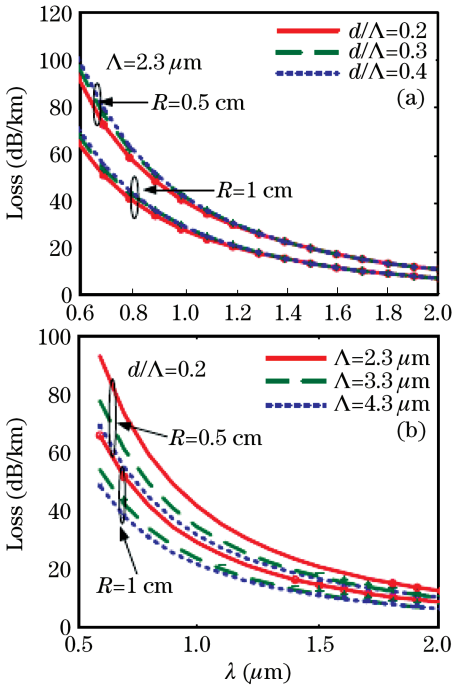

Fig. 8. Bending losses for $R = 1$ and 0.5 cm for (a) different d/Λ and (b) different Λ.

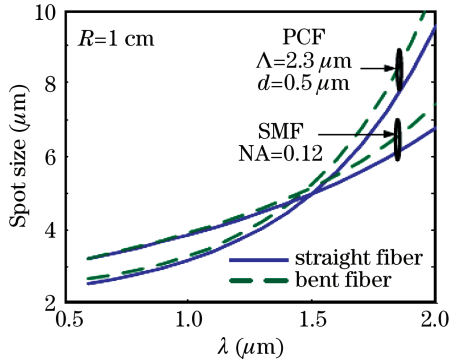

Fig. 9. Spot sizes of straight and bent SMF and PCF.

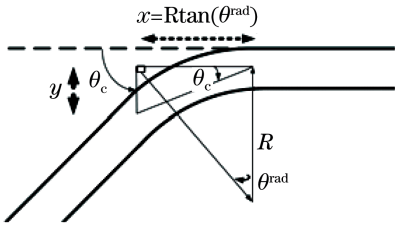

Fig. 10. Proposed Scheme.

The bending angle at the vicinity of the splice joint is shown in Fig. 10. From the geometry of the figure, we can derive the bending angle as

$$\theta = \arctan[y/(R\tan\theta^{\rm rad})],$$

$$\theta^{\rm rad} = \arcsin[(y/R)^2 - 1], \qquad (9)$$

where y is the bending length, having a maximum value of bending radius R.

The critical bending angle $\theta_{\rm c}$ is limited by the critical bending radius $R_{\rm c}$ obtained as

$$\theta_{\rm c} = \arctan[y/R\tan\{\arcsin(y^2/R_{\rm c}^2 - 1)\}]. \qquad (10)$$

By simultaneously adjusting the bending and the displacement at the splice joint, one can provide a condition to minimize the splice loss between PCF and SMF with different geometries.

In conclusion, a theoretical analysis of splice loss between PCF and SMF, using SEIM, VEIM, and FDFD methods is presented. The results show that a slight bending at the vicinity of splice joint causes a sharp increase in the spot size. Based on the results, a mechanism to optimize the splice loss between PCFs and SMFs, both with any geometry, is suggested.

The authors acknowledge the support of the Iran Telecom Research Center for Project 8631351.

References

1. P. J. Bennett, T. M. Monro, and D. J. Richardson, Opt. Lett. **24,** 1203 (1999).
2. G. E. Town and J. T. Lizier, Opt. Lett. **26,** 1042 (2001).
3. J. T. Lizier and G.E Town, IEEE Photon. Technol. Lett. **13,** 794 (2001).
4. B. Bourliaguet, C. Paré, F. Émond, and A. Croteau, A. Proulx, and R. Vallée, Opt. Express **11,** 3412 (2003).
5. A. D. Yablon and R. T. Bise, IEEE Photon. Technol. Lett. **17,** 118 (2005).
6. S. G. Leon-Saval, T. A. Birks, N. Y. Joly, A. K. George, W. J. Wadsworth, G. Kakarantzas, and P. St. J. Russell, Opt. Lett. **30,** 1629 (2005).
7. K. Saitoh, Y. Tsuchida, and M. Koshiba, Opt. Lett. **30,** 1779 (2005).

8. Y. Li, C. Wang, and M. Hu, Opt. Commun. **238,** 29 (2004).
9. Z. Zhu and T. G. Brown, Opt. Express **8,** 547 (2001).
10. F. E. Seraji, M. Rashidi, and V. Khasheie, Chin. Opt. Lett. **4,** 442 (2006).
11. J. C. Baggett, T. M. Monro, K. Furusawa, V. Finazzi, and D. J. Richardson, Opt. Commun. **227,** 317 (2003).
12. Z. Zhu and T. G. Brown, Opt. Express **10,** 853 (2002).
13. H. P. Uranus and H. J. W. M. Hoekstra, Opt. Express **12,** 2795 (2004).
14. S. Guo, F. Wu, S. Albin, H. Tai, and R. Rogowski, Opt. Express **12,** 3341 (2004).
15. A. K. Ghatak and K. Thyagarajan, *Introduction to Fiber Optics* (Cambridge University Press, Cambridge, 1998).
16. M. D. Nielsen, N. A. Mortensen, J. R. Folkenberg, and A. Bjarklev, Opt. Lett. **28,** 2309 (2003).
17. Corning Inc., "Corning SMF 28e+ optical fiber product information sheet" http://www.corning.com/opticalfiber/library (Feb. 25, 2007).
18. M. D. Nielsen, N. A. Mortensen, M. Albertsen, J. R. Folkenberg, A. Bjarklev, and D. Bonacinni, Opt. Express **12,** 1775 (2004).